

Analytical Methods

Accepted Manuscript



This is an *Accepted Manuscript*, which has been through the Royal Society of Chemistry peer review process and has been accepted for publication.

Accepted Manuscripts are published online shortly after acceptance, before technical editing, formatting and proof reading. Using this free service, authors can make their results available to the community, in citable form, before we publish the edited article. We will replace this *Accepted Manuscript* with the edited and formatted *Advance Article* as soon as it is available.

You can find more information about *Accepted Manuscripts* in the [Information for Authors](#).

Please note that technical editing may introduce minor changes to the text and/or graphics, which may alter content. The journal's standard [Terms & Conditions](#) and the [Ethical guidelines](#) still apply. In no event shall the Royal Society of Chemistry be held responsible for any errors or omissions in this *Accepted Manuscript* or any consequences arising from the use of any information it contains.

High-sensitive aptasensor for oxytetracycline based on upconversion and magnetic nanoparticles

Congcong Fang, Shijia Wu, Nuo Duan, Shaoliang Dai and

Zhouping Wang*

*State Key Laboratory of Food Science and Technology, Synergetic Innovation Center
of Food Safety and Nutrition, School of Food Science and Technology, Jiangnan
University, Wuxi 214122, China*

*Corresponding author. Tel & Fax: +86-510-85917023; E-mail: wangzp@jiangnan.edu.cn

Abstract

A novel sensitive aptasensor was developed for the quantification of oxytetracycline (OTC) in this study. Artificial aptamer-modified magnetic nanoparticles (aptamer-MNPs) were employed as capture probes, and complementary oligonucleotides modified upconversion nanoparticles (cDNA-UCNPs) were used as signal probes. Then, the probes were hybridized to form the poly-network structure MNPs-UCNPs signal probes. Finally, when the target was introduced, the aptamer combine with the target in priority and the signal probe was replaced. The proposed method achieved a linear range between 0.05 to 100 ng mL⁻¹, and the limits of detection (LOD) was as low as 0.036 ng mL⁻¹, benefiting largely from UCNPs labeling, aptamer affinity and magnetic separation. Then, we successfully applied the method to measure OTC in milk samples and validated it by a commercially available enzyme-linked immunosorbent assay (ELISA) method. The results demonstrated that the method possessed great sensitivity and good selectivity for the determination of OTC and is applicable to the determination of OTC in food samples.

Keywords: Aptamer; Oxytetracycline; Magnetic Nanoparticles; Upconversion Nanoparticles

1 Introduction

With a unique upconversion mechanism that enables the conversion of low-energy photons (near infrared photons) into high-energy photons (visible to ultraviolet photons) via multiphoton processes, lanthanide doped upconversion nanoparticles (UCNPs) have attracted enormous attention in the recent years¹⁻³. Upconversion nanoparticles possess tremendous advantages in biological applications over other types of fluorescent materials (e.g., organic dyes, fluorescent proteins, gold nanoparticles, quantum dots, and luminescent transition metal complexes)⁴, including low toxicity, large Stokes shifts, high quantum yields, high resistance to photo bleaching, blinking, photochemical stability and the lack of both auto-luminescence and a light scattering background, which consequently results in detection with high sensitivity and signal-to-noise ratio⁵⁻¹⁰. Meanwhile, magnetic nanoparticles (MNPs) with good biocompatibility and rapid separation from the substrate solution have been extensively implemented in the fields of biological detection¹¹⁻¹³.

Tetracyclines (TCs) are broad-spectrum antibiotics that include oxytetracycline, which is likely the most widely used antibacterial in aquaculture¹⁴. The presence of tetracycline residue especially oxytetracycline (OTC) from animal-derived foods poses a great risk towards human health, such as allergic reactions, toxic effects and the

1
2
3
4 development of resistance of microorganisms to antibiotics ^{15, 16}.
5
6 Therefore, researchers have made significant efforts to develop methods
7
8 to identify and quantify OTC, such as HPLC–DAD and LC–MS/MS ^{17, 18}.
9
10 Though sensitive and accurate, these methods demand expensive
11
12 equipment, tedious sample extraction procedures and technical skills ¹⁹.
13
14 Similarly, with wide range of application and low testing costs,
15
16 immunochemical methods using antibody usually lack specificity and
17
18 sensitivity due to the high similarity in structure of tetracycline
19
20 derivatives. In addition, the methods are unstable because the antibody is
21
22 sensitive to pH, temperature and other physicochemical environments in
23
24 biological samples ^{20, 21}. Therefore, it is still in demand to develop
25
26 sensitive and specific methods to detect OTC.
27
28
29
30
31
32

33
34 Aptamers are DNA or RNA molecules, which can adopt specific
35
36 three-dimensional conformations to combine with target analytes.
37
38 Compared with antibodies, aptamers are more stable, are easier to
39
40 synthesize, can be modified in bulk and have many other advantages ^{22, 23}.
41
42 To the author's knowledge, a series of aptasensors for OTC have been
43
44 developed ^{24, 30}. Though the reported electrochemical, colorimetric light
45
46 scattering and microcantilever methods should be highly sensitive, they
47
48 are of limited utility because of either high background signal or
49
50 instability in biological samples due to the inherent characteristics of the
51
52 nanoparticles used, and can be difficult to utilize for on-site detection
53
54
55
56
57
58
59
60

1
2
3 because of the tedious immobilization steps of the aptamers³¹. Therefore,
4
5
6 it is meaningful to overcome the above limitations and to search for a
7
8
9 simple and sensitive aptamer-based detection method for OTC.

10
11 Herein, we present an aptasensor for OTC based on upconversion
12
13 and magnetic nanoparticles, possessing excellent sensitivity and
14
15 selectivity, lacking in interference from auto-luminescence of other
16
17 biomolecules. Artificial aptamer-modified magnetic nanoparticles
18
19 (aptamer-MNPs) were employed as capture probes, and complementary
20
21 strand-modified upconversion nanoparticles (cDNA-UCNPs) were used
22
23 as signal probes. Then, the probes were hybridized to form the
24
25 poly-network structure MNPs-UCNPs signal probes. Finally, when the
26
27 target was introduced, the aptamer combined with the target in priority
28
29 and the signal probe was replaced. Thus, a novel analytical method has
30
31 been successfully applied to the detection of OTC relying on UCNP
32
33 labeling, aptamer selectivity and magnetic separation. Additionally, the
34
35 detection limit was as low as 0.036 ng·mL⁻¹. To our knowledge, this is the
36
37 first report to detect OTC using UCNPs and aptamer. □Furthermore, as
38
39 UCNPs can be doped with lanthanide ions, such as Er³⁺, Ho³⁺ and
40
41 Tm³⁺, this proposed method has great potential in the detection of
42
43 structurally similar tetracycline derivatives based on multicolor UCNPs.
44
45
46
47
48
49
50
51
52

53 54 **2 Experiments**

55 56 **2.1 Materials and chemicals**

57
58
59
60

1
2
3
4 The rare earth chloride and nitrates used in this work, including
5 $\text{YCl}_3 \cdot 6\text{H}_2\text{O}$, $\text{YbCl}_3 \cdot 6\text{H}_2\text{O}$, $\text{ErCl}_3 \cdot 6\text{H}_2\text{O}$, $\text{Y}(\text{NO}_3)_3 \cdot 6\text{H}_2\text{O}$, $\text{Yb}(\text{NO}_3)_3 \cdot 5\text{H}_2\text{O}$,
6 and $\text{Er}(\text{NO}_3)_3 \cdot 5\text{H}_2\text{O}$, were of 99.99% purity and were purchased from
7 Aladdin Industrial Inc. (Shanghai, China). Oleic acid, octadecene (ODE),
8 cyclohexane, 25% ammonia, 25% glutaraldehyde ($\text{OHC}(\text{CH}_2)_3\text{CHO}$),
9 Iron trichloride ($\text{FeCl}_3 \cdot 6\text{H}_2\text{O}$), tetraethyl orthosilicate (TEOS),
10 1,6-hexanediamine and ethanol were of analytical grade and were
11 purchased from Sinopharm Chemical Reagent Co., Ltd. (Shanghai, China).
12 IGEPAL CO-520, 98% 3-aminopropyltrimethoxysilane (APTES) was
13 purchased from Alfa Assar (USA). OTC aptamer (reported by Javed H.
14 Niazi. et al. ²²) and its partially complementary strand were synthesized
15 by Shanghai Sangon Biological Science & Technology Company
16 (Shanghai, China). The sequence of the OTA aptamer was
17 $5' \text{-NH}_2 \text{-GGAATTCGCTAGCACGTTGACGCTGGTGCCCGGTTGTGG}$
18 $\text{TGCGAGTGTTGTGTGGATCCGAGCTCCACGTG-3'}$ (aptamer), the
19 sequence of its partially complementary strand was
20 $5' \text{-NH}_2 \text{-CGGATCCACACAACA-3'}$ (cDNA). Oxytetracycline (OTC),
21 tetracycline (TET), and doxycycline (DOX) were purchased from
22 Aladdin Reagent Co., Ltd. (Shanghai, China).

2.2 Apparatus

23
24
25
26
27
28
29
30
31
32
33
34
35
36
37
38
39
40
41
42
43
44
45
46
47
48
49
50
51
52
53
54
55
56
57
58
59
60
The size and morphology of nanoparticles were observed on a
JEM-2100HR transmission electron microscope (TEM, JEOL Ltd.,

1
2
3
4 Japan), using a 200 kV accelerating voltage 200 kV. X-ray diffraction
5
6 (XRD) measurements were performed using a D8-advance instrument
7
8 (Bruker AXS Ltd., Germany) with graphite-mono-chromatized Cu-K α
9
10 radiation ($\lambda=0.15406$ nm). The luminescence spectra of UCNPs were
11
12 measured on an F-7000 luminescence spectrophotometer (Hitachi Co.,
13
14 Japan) attached to an external 980 nm laser (Beijing Hi-Tech
15
16 Optoelectronic Co., China) instead of the internal excitation source. The
17
18 maximum power of the laser was 1300 mW. FTIR spectra of the
19
20 amino-modified NPs were measured with a Nicolet Nexus 470 Fourier
21
22 transform infrared spectrophotometer (Thermo Electron Co., USA) using
23
24 the KBr method. Ultraviolet-visible (UV-vis) absorption spectra were
25
26 recorded using a Shimadzu UV-2300 UV-vis spectrophotometer
27
28 (Shimadzu, Japan) and concentration of oligonucleotides was measured
29
30 using the One Drop OD-1000 Spectrophotometer (OneDrop Technologies,
31
32 Inc., USA).
33
34
35
36
37
38
39
40

41 **2.3 Synthesis and surface modification of rare-earth-doped NaYF₄:** 42 43 **Yb, Er upconversion nanoparticles**

44
45
46 NaYF₄: 18% Yb, 2% Er UCNPs were synthesized by method
47
48 described by Zhengquan Li and Yong Zhang with some modifications³².
49
50 All of the doping ratios of Ln³⁺ ions are molar in our experiments. Briefly,
51
52 YCl₃, YbCl₃ and ErCl₃ were mixed with 6 mL of oleic acid and 17 mL of
53
54 octadecene in a 50 mL flask and heated to 160 °C to form a homogeneous
55
56
57
58
59
60

1
2
3
4
5
6
7
8
9
10
11
12
13
14
15
16
17
18
19
20
21
22
23
24
25
26
27
28
29
30
31
32
33
34
35
36
37
38
39
40
41
42
43
44
45
46
47
48
49
50
51
52
53
54
55
56
57
58
59
60

solution, and then cooled to room temperature. A 10 mL methanol solution containing NaOH and NH₄F was slowly added into the flask. The solution was stirred for 30 min, and the temperature was raised to evaporate the methanol; then, the solution was degassed at 100 °C for 10 min, before being heated to 300 °C and maintained for 1 h under argon atmosphere. After the solution was cooled, nanocrystals were precipitated from the solution with ethanol and washed with ethanol/water (1:1 v/v) three times.

Surface modification of NaYF₄: Yb, Er UCNPs was completed using a microemulsion method to cap silica onto the surface of the UCNPs³³. Then, 500 µl of CO-520 and 10 ml of cyclohexane containing NaYF₄ nanospheres were mixed and stirred for 10 min, then ammonia was added and the solution was sonicated for 20 min until a transparent emulsion was formed. TEOS and APTES were added to the solution, and the solution was rotated for two days at a speed of 600 rpm. Silica/NaYF₄ nanospheres were precipitated by adding acetone, and the nanospheres were washed with ethanol/water.

2.4 Preparation of amino-modified Fe₃O₄ magnetic nanoparticles (MNPs)

To prepare MNPs, a one-pot synthetic method was adopted³⁴. For ~25 nm magnetic nanoparticles, a solution of 1, 6-hexanediamine (6.5 g),

1
2
3
4 anhydrous sodium acetate (2.0 g) and $\text{FeCl}_3 \cdot 6\text{H}_2\text{O}$ (1.0 g) as a ferric
5
6 source in glycol (30 mL) was stirred vigorously to give a transparent
7
8 solution. This solution was then transferred into a Teflon-lined autoclave
9
10 and reacted at 198 °C for 6 h. The magnetic nanoparticles were then
11
12 rinsed with water and ethanol (2 or 3 times) to effectively remove the
13
14 solvent and unbound 1, 6-hexanediamine and then dried before
15
16 characterization and application. During each rinsing step, the
17
18 nanoparticles were separated from the supernatant by using magnetic
19
20 force.
21
22
23
24
25

26 **2.5 Preparation of signal probes and capture probes**

27

28
29 The procedure for the preparation of oligonucleotides conjugated
30
31 MNPs and UCNPs was adapted from the classical glutaraldehyde method
32
33 ³⁵. 10 mg of the amino-modified nanoparticles was dispersed in 5 mL of
34
35 phosphate buffer solution (PBS) at pH 7.4 by ultrasonication for 15 min,
36
37 and then 0.2 mL of 25% glutaraldehyde was added into the mixture. The
38
39 mixture was shaken slowly on a shaking table at room temperature for 2 h.
40
41 After incubation, the MNPs were separated with an external magnetic
42
43 field and the UCNPs were separated by centrifugation. The nanoparticles
44
45 were washed with phosphate buffer solution three times and dispersed in
46
47 5 mL of PBS buffer solution.
48
49
50
51
52

53
54 Then, amino-modified aptamer was subsequently added to the
55
56 glutaraldehyde modified MNPs and amino-modified cDNA was added to
57
58
59
60

1
2
3
4 the glutaraldehyde modified UCNPs. The mixture was then incubated at
5
6 37°C for another 2 h. After removal of the supernatant and washing, the
7
8 resulting solution was resuspended in fresh STE buffer (10 mM Tris-HCl,
9
10 pH 8.0, 50 mM NaCl, 1 mM EDTA) and stored at 4 °C.

11 12 13 14 **2.6 Procedure for the detection of OTC**

15
16 A total of 100 µL of aptamers-MNPs was hybridized in STE buffer
17
18 with the optimized cDNA-UCNPs at 37 °C for 2 h to obtain
19
20 UCNPs-MNPs signal probes. The UCNPs-MNPs probes were separated
21
22 by a magnetic field and were resuspended in PBS buffer. Then various
23
24 concentrations of OTC standard were added to the mixture and further
25
26 incubated at 37 °C for 2 h. The remaining UCNPs-MNPs were then
27
28 separated and washed three times, and the luminescence intensity was
29
30 measured with a 980 nm excitation laser.

31 32 33 34 35 36 **2.7 Method comparison with ELISA analysis in food samples and** 37 38 **recovery experiment**

39
40 The accuracy of OTC detection in food samples was evaluated by
41
42 determining the recovery of OTC (Recovery ratio = (Detected
43
44 Concentration - Background Content) / Added Concentration). Briefly, a
45
46 series of known quantities of OTC standard were added into the milk
47
48 samples. And the milk samples were pretreated with centrifugation
49
50 separation (10 °C, 3500 r·min⁻¹) for 10 min. Next, the supernatant was
51
52 collected and diluted with PBS buffer proportionately (1:10 v/v). Finally,
53
54
55
56
57
58
59
60

1
2
3
4 the OTA content of the resulting solution was measured with the
5
6 developed aptasensor by the above mentioned procedure. Furthermore,
7
8 the commercially available ELISA method was also applied to detect the
9
10 OTC in the same milk samples.
11
12

13 **3 Results and discussion**

14 **3.1 Detection principle**

15
16
17 The luminescence bioassay platform for the detection of OTC based
18
19 on upconversion and magnetic nanoparticles was illustrated in Fig. 1.
20
21 Specifically, amino-modified MNPs were conjugated with
22
23 amino-modified aptamer via the classical glutaraldehyde method ³⁵ to
24
25 form the capture probes (aptamer-MNPs), and amino-modified NaYF₄:
26
27 Yb, Er UCNPs were conjugated with amino-modified cDNA to form the
28
29 signal probes (cDNA-UCNPs). Then, the probes were hybridized to form
30
31 the MNPs-UCNPs signal probes.
32
33
34
35
36
37

38
39 After magnetic separation with an external magnet, the intensity of
40
41 the emission peak at 544 nm was at a maximum in the absence of OTC,
42
43 because of the abundance of the MNPs-UCNPs signal probes.
44
45 Subsequently, OTC was added to the system, and aptamer preferentially
46
47 bound to OTC caused the dissociation of some cDNA, thereby liberating
48
49 some cDNA-UCNPs. Finally, the intensity of the emission peak at 544
50
51 nm decreased as a result of the reduced concentration of MNPs-UCNPs
52
53 signal probes.
54
55
56
57
58
59
60

3.2 Design of complementary DNA sequences

In this study, we experiment with a sequence of the partially complementary strand of the aptamer 5'-NH₂-CGGATCCACACAACA-3'. The basic principle of the cDNA design was that aptamers could form a defined conformation when conjugating to the targets and were also able to hybridize to the cDNA to form a duplex structure³⁶⁻³⁷. While designing oligonucleotides strand of cDNA, proper care was taken to avoid excessive adhesive strength with the aptamer. When the targets and the complementary oligonucleotides were introduced, the aptamers preferentially bound to the targets, resulting in the specific recognition of the targets³⁸⁻³⁹.

3.3 Preparation and characterization of UCNPs

The UCNPs were synthesized via a solvothermal method using chloride. Transmission electron microscopy (TEM) images of the nanocrystals in Fig. 2 (a-b) show the size and morphology of the oleic acid-capped UCNPs. The NPs were then coated by the microemulsion method and characterized by the TEM at the same time.

In this work, uniform NaYF₄ nanospheres with strong upconversion luminescence were produced, with uniform silica coating on the surface. The microemulsion method has been one of the most commonly used methods for coating silica on nanocrystals. However, it is quite challenging to coat individual nanoparticles with very thin shells. Thus,

1
2
3
4 we have optimized the microemulsion method by adding different
5
6 proportions of UCNPs and TEOS, and finally resulted in the thickness of
7
8 silica shell with approximately 2 nm (Fig. 2 c-d). By shortening the
9
10 reaction time and increasing the UCNPs concentration, it is possible to
11
12 create somewhat thinner layers of silica. After silica coating, the
13
14 nanocrystals were dispersible in water and demonstrated good chemical
15
16 and photochemical stability. Fig. 3 shows the luminescence intensity is
17
18 only slightly reduced with the thin silica shell on the surface.
19
20
21
22

23
24 NaYF₄: Yb, Er nanocrystals have been shown to be the best
25
26 NIR-to-visible upconversion luminescence materials and
27
28 hexagonal-phase nanocrystals have higher upconversion efficiency than
29
30 cubic-phase nanocrystals³². Fig. 4 gives the XRD patterns of NaYF₄: Yb,
31
32 Er UCNPs, revealing the prepared UCNPs are pure hexagonal-phase
33
34 (JCPDS no. 16-0334).
35
36
37
38

39 In addition to fabricating thin and uniform silica shells, the UCNPs
40
41 were furthermore functionalized with APTES to form an
42
43 amino-terminated surface. The functional groups on the surfaces of the
44
45 amino-modified NaYF₄: Yb, Er UCNPs were identified by FT-IR spectra
46
47 in Fig. 5. The wide absorption peak at 3412 cm⁻¹ in Fig. 5 a is the
48
49 stretching vibration of the hydroxyl group. Two peaks found at 1560 and
50
51 1458 cm⁻¹ correspond to the asymmetric and symmetric stretching
52
53 vibrations of the carboxylic group (COO⁻). In addition, bands at 2921
54
55
56
57
58
59
60

1
2
3
4 and 2853 cm^{-1} are assigned to the asymmetric and symmetric stretching
5
6 vibrations of the methylene group, respectively, caused by the long chain
7
8 alkyl from oleic acid molecules. The results verified the UCNPs before
9
10 modifying were coated by oleic acid molecules. In contrast, the peaks
11
12 mentioned above disappeared together in Fig. 5 b, and the characteristic
13
14 peaks corresponding to amino groups appeared instead. The hydroxyl
15
16 stretching vibration band of a silanol group (Si–OH) appears in the region
17
18 approximately 3402 cm^{-1} , and the band at 1068 cm^{-1} is attributed to the
19
20 stretching vibration of the Si–O bond. The spectrum at 1625 cm^{-1} is the
21
22 stretching and bending vibration bands of the amino group indicating that
23
24 the silica-coated UCNPs have been successfully functionalized with
25
26 amino groups.
27
28
29
30
31
32

33 34 **3.4 Preparation and characterization of MNPs**

35
36 The amino-modified Fe_3O_4 MNPs applied here were prepared by a
37
38 one-pot synthesis. TEM (Fig. 6 a) and FT-IR (Fig. 6 b) are used to
39
40 characterize the synthesized MNPs. It can be observed that the MNPs
41
42 have an average size of approximately 25 nm. FT-IR spectroscopy shows
43
44 a strong IR band at 583 cm^{-1} , which is characteristic of the Fe–O
45
46 vibrations. The transmissions at approximately 1634, 1396, and 1054
47
48 cm^{-1} from the amino-modified nanoparticles matched well with those
49
50 from free 1,6-hexanediamine, indicating the existence of the free $-\text{NH}_2$
51
52 group on the amino-modified nanomaterials. The results from FT-IR
53
54
55
56
57
58
59
60

1
2
3 revealed that the MNPs have been functionalized with amino groups in
4 the synthetic process.
5
6
7

8 **3.5 Characterization of amino-modified nanoparticles conjugated** 9 **with amino-modified oligonucleotides** 10 11

12 We applied UV-vis spectrophotometry to validate successfully
13 coupling of amino-modified oligonucleotides to amino-modified
14 nanoparticles. As is shown in Fig. 7, the strong absorbance of
15 oligonucleotides can be seen at 260 nm before conjugation to
16 nanoparticles. After incubation of amino-modified nanoparticles and
17 amino-modified oligonucleotides, the supernatant was collected by
18 magnetic separation and centrifugation. The absorbance of the
19 supernatant liquor was weaker at 260 nm with the decrease of peak
20 intensity since part of the oligonucleotides has been combined with
21 amino-modified nanoparticles.
22
23
24
25
26
27
28
29
30
31
32
33
34
35
36
37
38

39 We further determined the number of oligonucleotides conjugated on
40 nanoparticles applying the One Drop OD-1000 Spectrophotometer.
41 Initially, the concentration of aptamer was $179 \text{ ng } \mu\text{L}^{-1}$, and the
42 concentration of aptamer in the supernatant liquor collected after
43 incubating with the MNPs (2 mg ml^{-1}) decreased to $35 \text{ ng } \mu\text{L}^{-1}$, indicating
44 the conjugation yield between aptamer and MNPs was 77000 ng mg^{-1} .
45
46
47
48
49
50
51
52
53
54
55
56
57
58
59
60

1
2
3
4 was 49000 ng mg⁻¹.
5

6 **3.6 Optimize the dosage of probes**

7

8
9 To identify the optimal dosages of cDNA-UCNPs and
10 aptamer-MNPs, a comparative study was performed to reach a maximum
11 background luminescence of UCNPs-MNPs probes. A total of 100 μ L of
12 aptamer-MNPs and various volumes of cDNA-UCNPs solution was
13 hybridized together. As shown in Fig. 8, the luminescence intensity
14 increased with the dose of cDNA-UCNs solution increasing, and the
15 luminescence intensity reach maximum with the addition of 800 μ L of
16 cDNA-UCNPs solution. Initially, only a small quantity of UCNPs-MNPs
17 was fabricated as the low concentration of cDNA-UCNPs led to the
18 abundance of Apt-MNPs not having any cDNA-UCNPs to bind. When
19 the concentration of cDNA-UCNPs and the concentration of Apt-MNPs
20 were matched, the luminescence intensity reached a maximum. However,
21 if the quantity of cDNA-UCNPs was in excess, the luminescence
22 intensity of the UCNPs-MNPs decreased because the cDNA-UCNPs
23 were unable to combine with more aptamer-MNPs. The MNPs-UCNPs
24 obtained at the optimal dosages formed relatively stable suspension in
25 buffer as is shown in Fig. 9 a. And Fig. 9 b shows the MNPs-UCNPs
26 suspension emits green luminescence when excited by a 980 nm
27 excitation laser.
28
29
30
31
32
33
34
35
36
37
38
39
40
41
42
43
44
45
46
47
48
49
50
51
52
53
54
55

56 Furthermore, we measured the luminescence intensity of the
57
58
59
60

1
2
3
4 cDNA-UCNPs to determine the conjugation yield between Apt-MNPs
5 and cDNA-UCNPs. The black line in Fig. 10 was the luminescence
6 Spector of the 800 μL of cDNA-UCNPs solution before hybridizing with
7
8 100 μL Apt-MNPs together. After hybridization of Apt-MNPs and
9
10 cDNA-UCNPs, the supernatant was collected by magnetic separation and
11
12 was measured with a 980 nm excitation laser. As is shown in Fig. 10, the
13
14 intensity of the emission peak at 544 nm was reduced by about 41%,
15
16 since part of the cDNA-UCNPs has been combined with amino-modified
17
18 nanoparticles.

25 26 **3.7 Optimize the washing time**

27
28 After complete reaction between OTC and UCNPs-MNPs, the
29
30 cDNA-UCNPs dissociated from UCNPs-MNPs should be washed
31
32 thoroughly to prevent the interference. Therefore, we optimize the
33
34 washing time to reach the best washing effect. The UCNPs-MNPs probes
35
36 were exposed to OTC (10 ng mL^{-1}) and only buffer without OTC
37
38 respectively. The remaining UCNPs-MNPs were then separated an
39
40 external magnetic field and washed three times and the luminescence
41
42 intensity was measured with a 980 nm excitation laser. The results are
43
44 shown in Fig. 11, the luminescence intensity decreased with each
45
46 washing time increasing, and the remained constant when the washing
47
48 time was 15 s.

55 56 **3.8 Determination of OTC**

1
2
3
4
5
6
7
8
9
10
11
12
13
14
15
16
17
18
19
20
21
22
23
24
25
26
27
28
29
30
31
32
33
34
35
36
37
38
39
40
41
42
43
44
45
46
47
48
49
50
51
52
53
54
55
56
57
58
59
60

In this experiment, the luminescence intensity was at a maximum before the OTC was in absence. When the target molecule was introduced, the luminescence intensity decreased gradually as the aptamers preferentially bound to OTC and caused the dissociation of some cDNA-UCNPs from UCNPs-MNPs. Various intensities of luminescence spectra obtained in the presence of different concentrations of OTC are shown in Fig. 12 a. Fig. 12 b shows the linear relationship between the intensity of the upconversion luminescence and the concentration of OTC. The LOD of the aptasensor for OTC is as low as 0.036 ng mL^{-1} (calculated by the function of $3s/S$, where s is the standard deviation of the blank solution and S is the slope of the linear relationship). The precision expressed by the relative standard deviation (RSD) of OTC detection is 3.71% (10 ng mL^{-1} , $n = 10$). Table 1 presents some of the latest detection methods reported in recent years for OTC, which suggests that the proposed method is more sensitivity than most of those previously described.

Furthermore, we applied TEM to observe the morphology of MNPs-UCNPs before and after target treating. Fig. 13 a shows the morphology of MNPs-UCNPs before target treating. After OTC was added to the system, aptamer preferentially bound to OTC causing the dissociation of some cDNA, thereby liberating some cDNA-UCNPs. And Fig. 13 b shows the morphology of MNPs-UCNPs after target treating.

3.9 Specificity

Three structurally similar tetracycline derivatives, including OTC, DOX, and TET were used to verify the good selectivity of this method. The aptasensor were exposed to the derivatives, with the same concentration (10 ng mL^{-1}). The results are shown in Fig. 14, OTC caused a dramatic luminescence change as is respected, while the others failed. The good specificity of this method was attributed to the inherent specificity of aptamer toward OTC.

3.10 Analytical application

The accuracy of OTC detection in food samples was evaluated by determining the recovery of OTC by adding a series of known quantities of OTC into the milk samples. As shown in Table 2, the recoveries were between 98.60 % and 119.00 %, and there is no significant difference ($P < 0.0001$) between the results obtained by the aptasensor and ELISA method in Fig. 15, indicating the proposed aptamer-based bioassay can be applied for OTC detection in food samples.

4 Conclusions

In this study, a high-sensitive aptasensor for the rapid, and specific detection of OTC based on upconversion and magnetic nanoparticles was successfully developed and evaluated. Typically, the use of UCNPs avoided the auto luminescence originating from the biomolecules possibly contained in the solution entirely as the UCNPs were excited by

1
2
3
4 infrared 980 nm laser. Furthermore, the magnetic separation simplified
5
6 the experimental processes as the magnetic nanoparticles can concentrate
7
8 and separate targets from the food solution easily and rapidly. Lastly, the
9
10 aptamers were stable compared to traditional antibodies and highly
11
12 specific to the target OTC. In summary, the aptasensor offers a new
13
14 approach of convenience, sensitivity, specificity, and stability to detect
15
16 OTC in food samples.
17
18
19

20 21 **Acknowledgments**

22
23 This work was partly supported by the National S&T Support
24
25 Program of China (2012BAK08B01), NSFC (21375049), S&T
26
27 Supporting Project of Jiangsu Province (BE2011621, BE2012614),
28
29 JSCIQ_2012IK166, Research Fund for the Doctoral Program
30
31 of Higher Education (20110093110002), NCET-11-0663, and
32
33 JUSRP51309A.
34
35
36
37

38 39 **References**

- 40
41 1. C. Liu, H. Yi and M. Gao, *Adv. Mater.*, 2014.
42
43 2. P. Wang, P. Joshi, A. Alazemi and P. Zhang, *Boosens. Bioelectron.*,
44
45 2014, **62**, 120–126.
46
47 3. A. Xia, X. Zhang, J. Zhang, Y. Deng, Q. Chen, S. Wu, X. Huang and J.
48
49 Shen, *Biomaterials*, 2014, **35**, 9167-9176.
50
51 4. Z. Gu, L. Yan, G. Tian, S. Li, Z Chai and Y. Zhao, *Adv. Mater.*, **25**,
52
53 3758-3579.
54
55
56
57
58
59
60

- 1
2
3
4 5. Q. Zhan, S. He, J. Qian, H. Cheng and F. Cai, *Theranostics*, 2013, **3**,
5
6 306-316.
7
- 8
9 6. Y. Zhai, C. Zhu, J. Ren, E. Wang and S. Dong, *Chem. Commu.*, 2013,
10
11 **49**, 2400-2402.
12
- 13
14 7. F. Lin, B. Yin, C. li, J. Deng, X. Fan, Y. Yi, C. Liu, H. Li, Y. Zhang
15
16 and S. Yao, *Anal. Methods*, 2013, **5**, 699.
17
- 18
19 8. X. Li, Z. Li, W. Gan, T. Wang, S. Zhao, Y. Lu, J. Cheng and G. Huang,
20
21 *Analyst*, 2013, **138**, 3711-3718.
22
- 23
24 9. S. Hao, G. Chen and C. Yang, *Theranostics*, 2013, **3**, 331-345.
25
- 26
27 10. L. Cheng, C. Wang, X. Ma, Q. Wang, Y. Cheng, H. Wang, Y. Li and
28
29 L. Zhuang, *Adv. Funct. Mater.*, 2013, **23**, 272-280.
30
- 31
32 11. S. Wu, N. Duan, C. Zhu, X. Ma, M. Wang and Z. Wang, *Biosens.*
33
34 *Bioelectron.*, 2011, **30**, 35-42.
35
- 36
37 12. S. Wu, N. Duan, Z. Wang and H. Wang, *Analyst*, 2011, **136**,
38
39 2306-2314.
40
- 41
42 13. Z. Huang, S. Wu, N. Duan, D. Hua, Y. Hu and Z. Wang, J.
43
44 *Pharmaceut. Biomed.* 2012, **66**, 225-231.
45
- 46
47 14. S. Graslund, and B.-E. Bengtsson, *Sci. Total Environ.*, 2001, **280**,
48
49 93-131.
50
- 51
52 15. A. Stolker and U. Brinkman, *J. Chromatogr. A*, 2005, **1067**,15-53.
53
- 54
55 16. S. A. de Albuquerque Fernandes, A. P. Magnavita, S.P. Ferrao, S. A.
56
57 Gualberto, A. S. Faleiro, A. J. Figueiredo and S. V. Matarazzo,
58
59
60

- 1
2
3
4
5
6
7
8
9
10
11
12
13
14
15
16
17
18
19
20
21
22
23
24
25
26
27
28
29
30
31
32
33
34
35
36
37
38
39
40
41
42
43
44
45
46
47
48
49
50
51
52
53
54
55
56
57
58
59
60
- Environ. Sci. Pollur.*, 2014, **21**, 3427-3434.
17. Á. Tölgyesi, L. Tölgyesi, K. Békési, V. K. Sharma and J. Fekete,
Meat. Sci., 2014, **96**, 1332-1339.
18. K. Škrášková, L. H. Santos, D. Šatínský, A. Pena, M. C. Montenegro,
P. Solich and N. Nováková, *J. Chromatogr. B*, 2013, **927**:201-208.
19. C.-H. Kim, L.-P. Lee, J.-R. Min, M.-W. Lim and S.-H. Jeong,
Biosens. Bioelectron., 2014, **51**, 426-430.
20. T. Wongtangprasert, W. Natakathung, U. Pimpitak, A. Buakeaw, T.
Palaga and K, *Journal of Zhejiang University Science B*, 2014, **15**,
165-172.
21. N. Ajami, N. Bahrami Panah and I. Danaee, *Iran Polym. J*, 2013,
23,121-126.
22. W. Yun, H. Li, S. Chen, D. Tu, W. Xie and Y. Huang, *Eur. Food Res.*
Technol., 2014, **238**, 989–995.
23. X. Ma, W. Wang, X. Chen, Y. Xia, S. Wu, N. Duan and Z. Wang, *Eur.*
Food Res. Technol., 2014, **238**, 919–925.
24. D. Zheng, X. Zhu, X. Zhu, B. Bo, Y. Yin and G. Li, *Analyst*, 2013,
138,1886-1890.
25. J. H. Niazi, S. J. Lee, Y. S. Kim and M. B. Gu , *Bioorga. Med. Chem.*,
2008, **16**, 1254-1261.
26. Y. S. Kwon, N. H. Ahmad Raston and M. B. Gu, *Chem. Commu.*,
2014, **50**, 40-42.

- 1
2
3
4 27. Y. S. Kim, J. H. Niazi and M. B. Gu, *Anal. Chim. Acta.*, 2009, **634**,
5 250-254.
6
7
8
9 28. Y. S. Kim, J. H. Kim, I. A. Kim, S. J. Lee, J. Jung and M. B. Gu,
10 *Biosens. Bioelectron.*, 2010, **26**, 1644-1649.
11
12
13 29. K. Kim, M. B. Gu, D. H. Kang, J. W. Park, I. H. Song, H. S. Jung and
14 K. Suh, *Electrophoresis*, 2010, **31**, 3115-3120.
15
16
17
18 30. H. Hou, X. Bai, C. Xing, N. Gu, B. Zhang and J. Tang, *Anal. Chem.*,
19 2013, **85**, 2010-2014.
20
21
22
23 31. H. Zhao, S. Gao, M. Liu, Y. Chang, X. Fan and X. Quan, *Microchimi.*
24 *Acta.*, 2013, **180**, 829-835.
25
26
27
28 32. Z. Li and Y. Zhang, *Nanotech.*, 2008, **19**, 345606.
29
30
31 33. Z. Li, Y. Zhang and S. Jiang, *Adv. Mater.*, 2008, **20**, 4765-4769.
32
33
34 34. L. Wang, J. Bao, L. Wang, F. Zhang and Y. Li, *Chem.*, 2006, **12**,
35 6341-6347.
36
37
38 35. X. Hun and Z. Zhang, *Biosens. Bioelectron.*, 2007, **22**, 2743-2748.
39
40
41 36. N. Hamaguchi, A. Ellington and M. Stanton, *Anal. Biochem.*, 2001,
42 **294**, 126-131.
43
44
45 37. R. Nutiu and Y. Li, *J. Am. Chem. Soc.*, 2003, **125**, 4771-4778.
46
47
48 38. W. U. Dittmer, A. Reuter and F. C. Simmel, *Angew. Chem., Int. Ed.*,
49 2004, **43**, 3550-3553.
50
51
52 39. Y. Xiao, B. D. Piorek, K. W. Plaxco and A. J. Heeger, *J. Am. Chem.*
53 *Soc.*, 2005, **127**, 17990-17991.
54
55
56
57
58
59
60

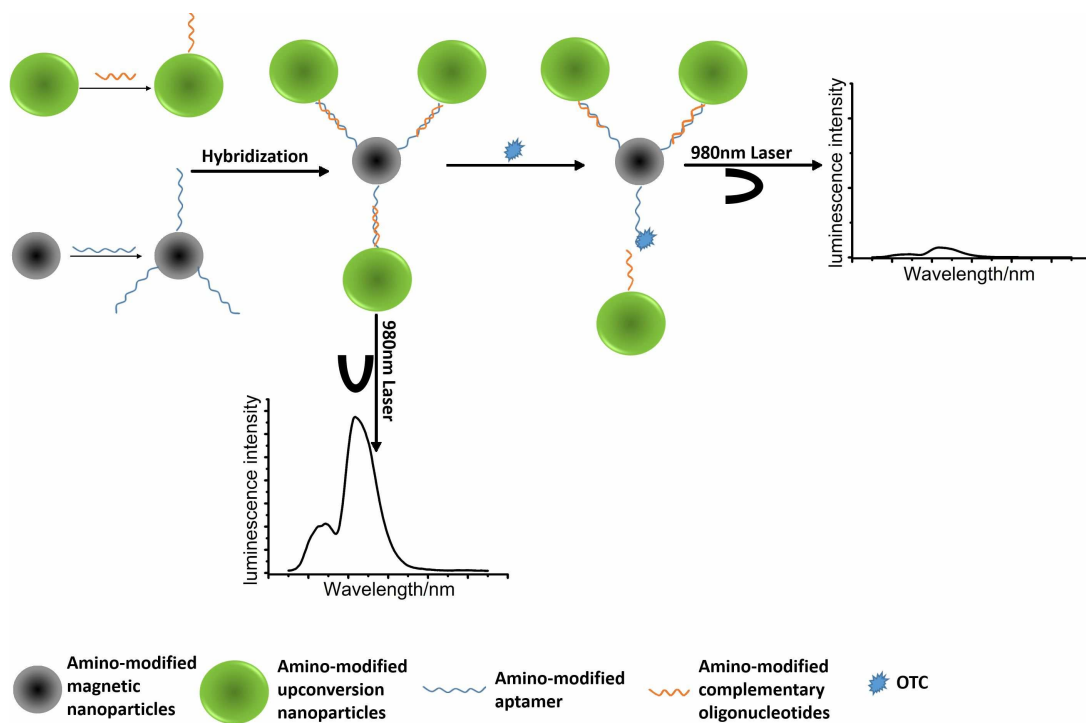


Fig. 1 Schematic illustration of the highly sensitive aptasensor for oxytetracycline based on upconversion and magnetic nanoparticles

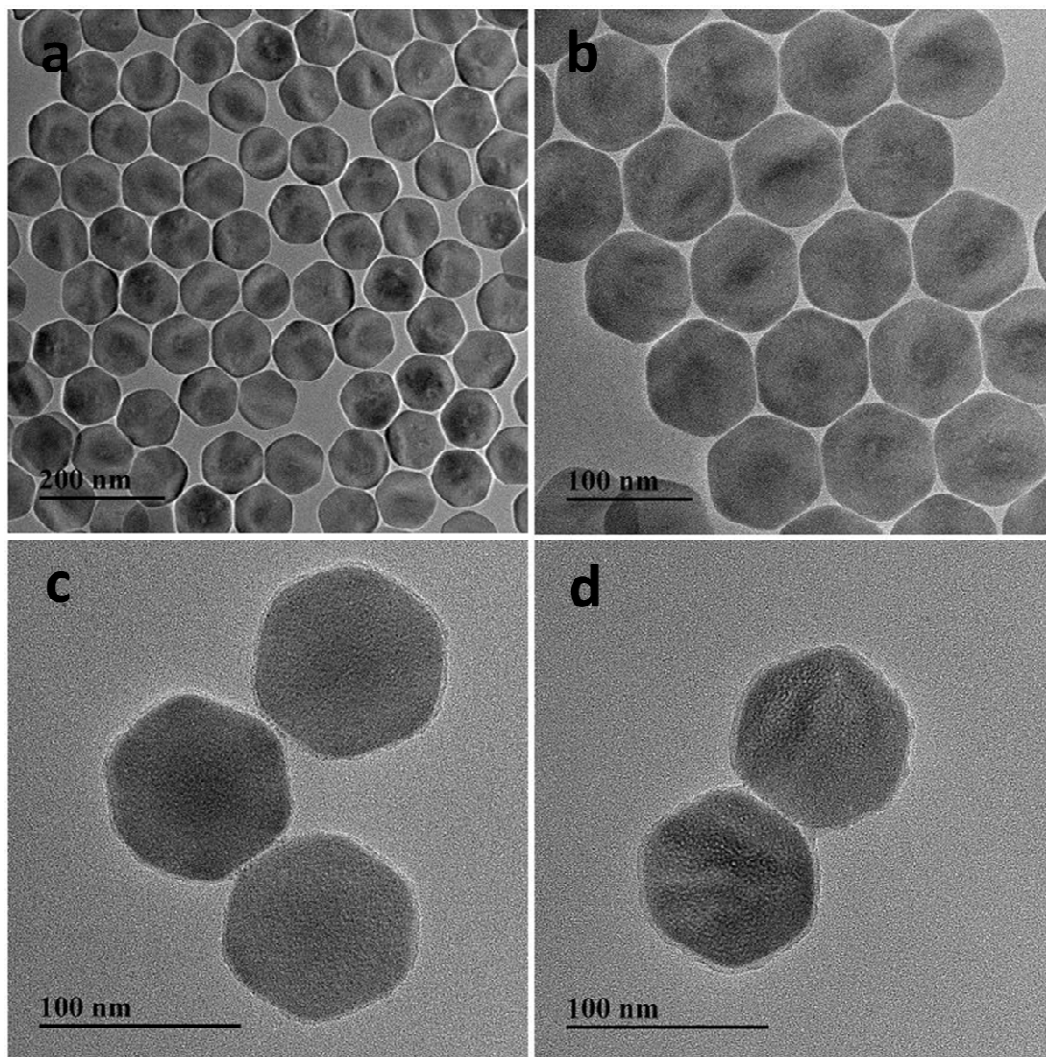


Fig. 2 TEM images of $\text{NaY}_{0.78}\text{F}_4: \text{Yb}_{0.20}, \text{Er}_{0.02}$ UCNPs before coating silica (a-b) and after coating silica (c-d)

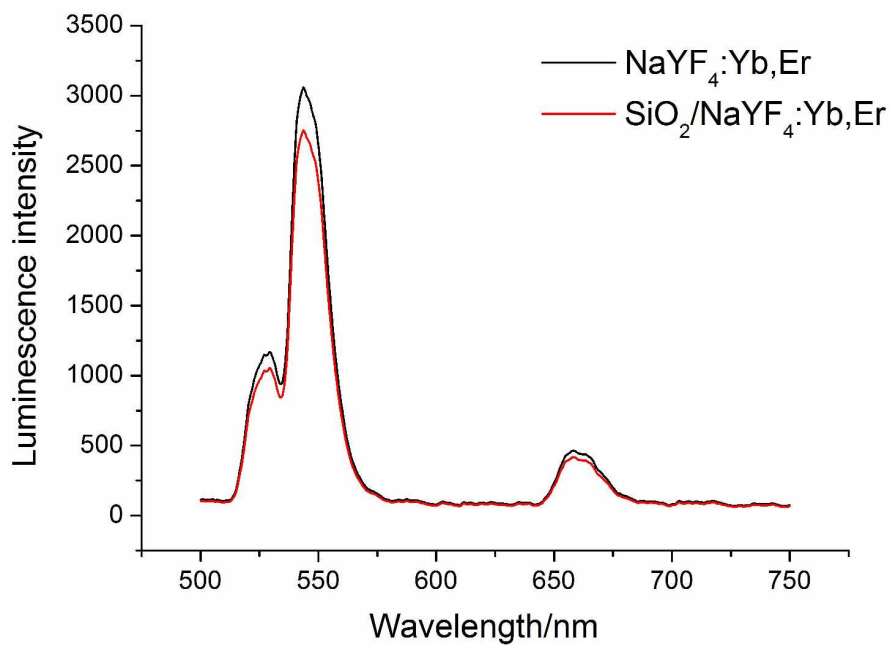


Fig. 3 Luminescence spectra of NaYF₄: Yb, Er nanospheres, with and without silica coating

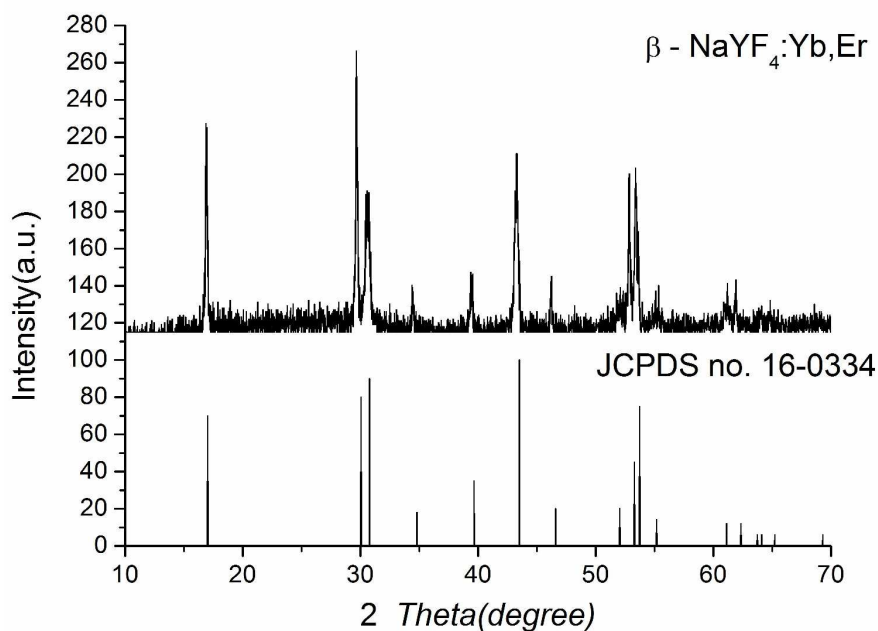


Fig. 4 XRD patterns of NaYF₄: Yb, Er UCNP synthesized via method 1 (a) and method 2 (b)

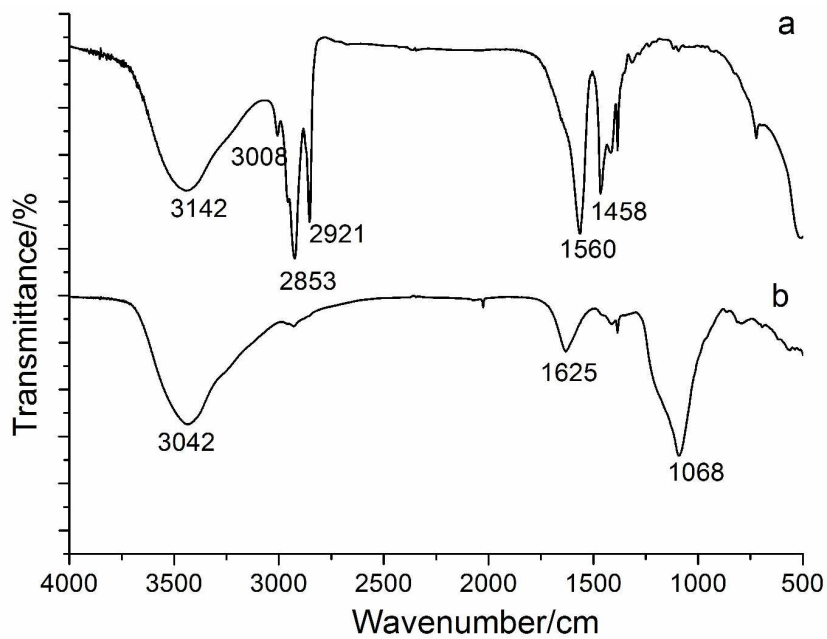


Fig. 5 FT-IR spectra without silica shells (a) and with silica shells (b)

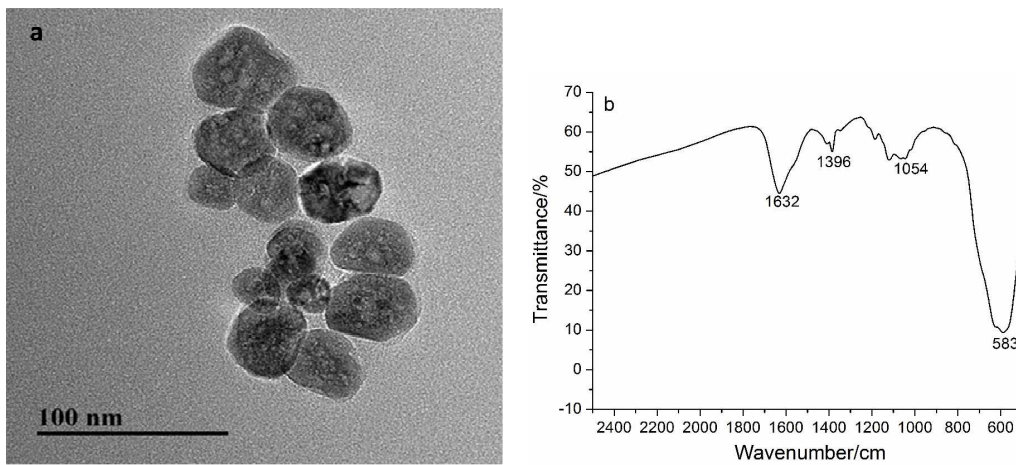


Fig. 6 TEM image (a) and FT-IR spectrum (b) of the amino-modified Fe₃O₄ nanoparticles

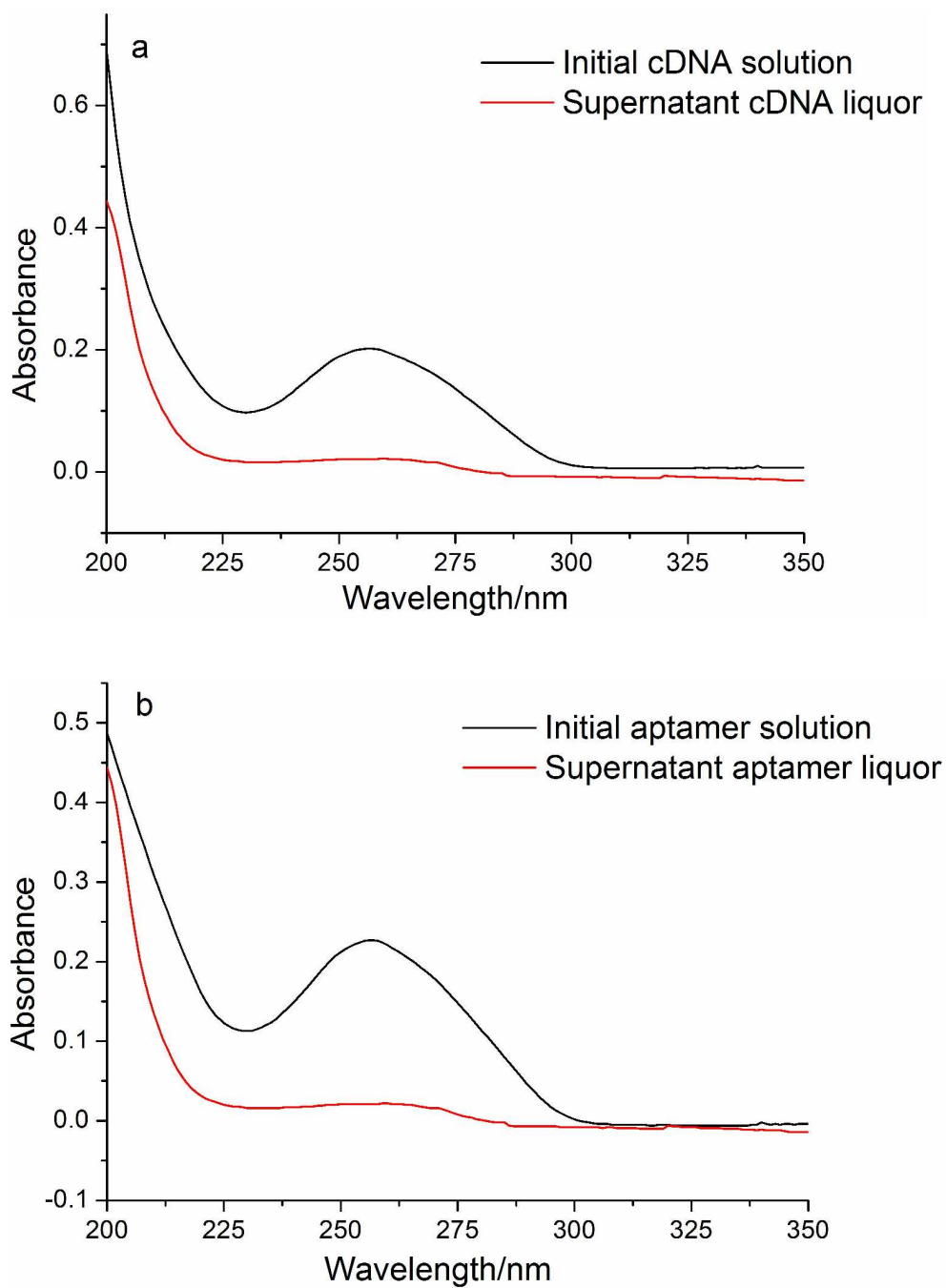


Fig. 7 UV-vis absorption spectra of cDNA solution (a) and aptamer solution (b) before and after conjugating with amino-modified nanoparticles (2mg ml^{-1})

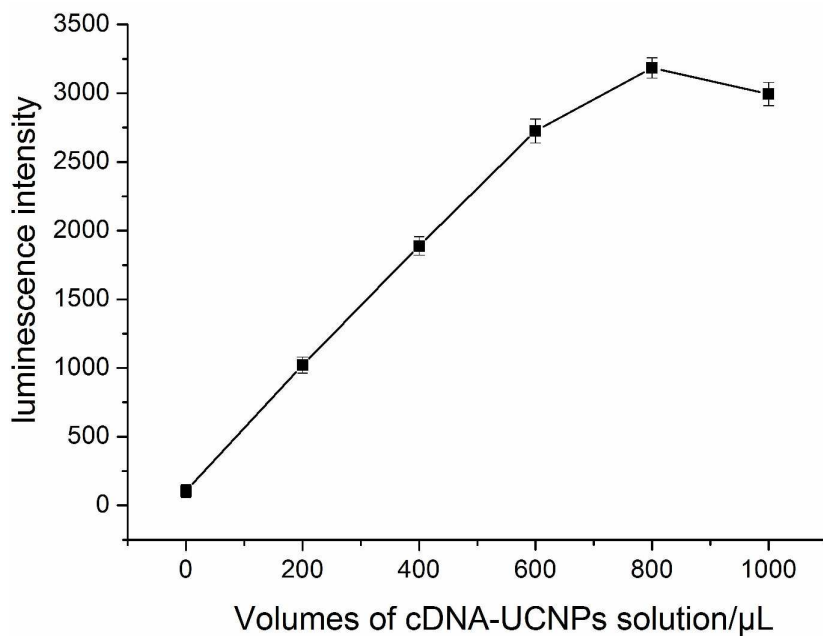


Fig. 8 Luminescence intensity of various volumes of cDNA-UCNPs (2 mg ml^{-1}) incubated with $100 \mu\text{L}$ of aptamer-MNPs (2 mg ml^{-1})



Fig. 9 The photographs of MNP-UCNPs suspension (a) and the luminescence of the suspension excited by a 980 nm excitation laser (b)

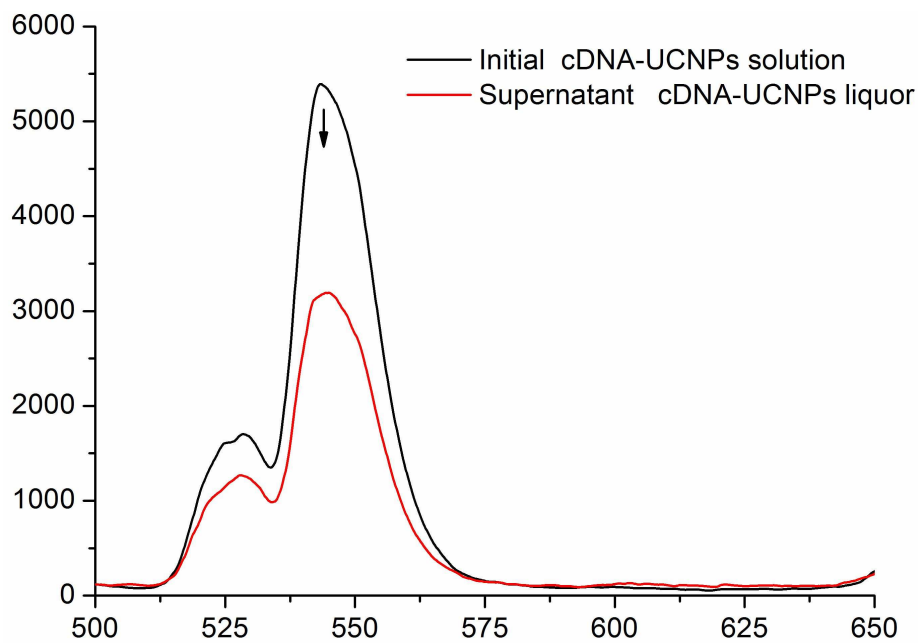


Fig. 10 Luminescence spectra of cDNA-UCNPs nanospheres (2 mg ml^{-1}) before and after hybridizing with $100 \mu\text{L}$ of Apt-MNPs (2 mg ml^{-1})

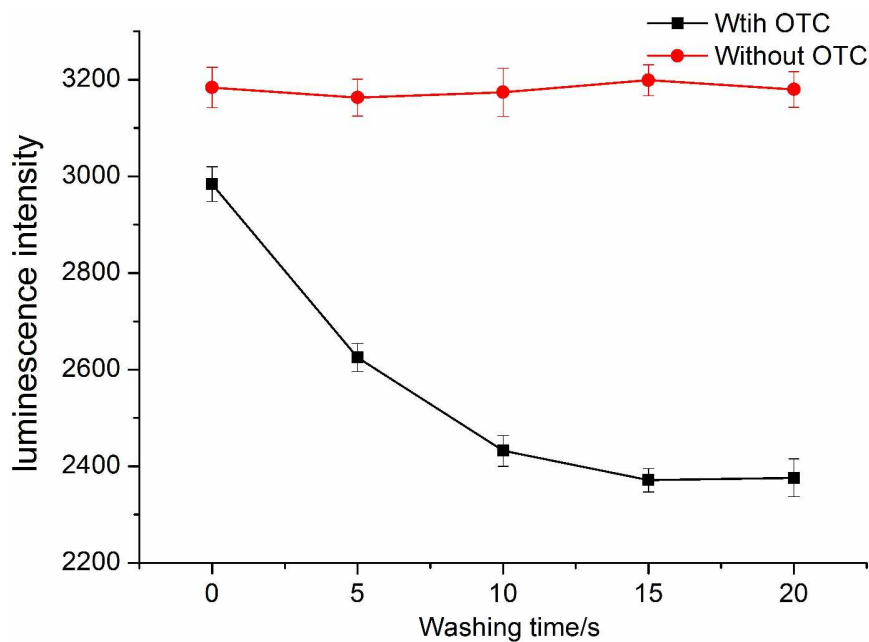


Fig. 11 Luminescence intensity of various washing time with OTC (10 ng ml^{-1}) and without OTC

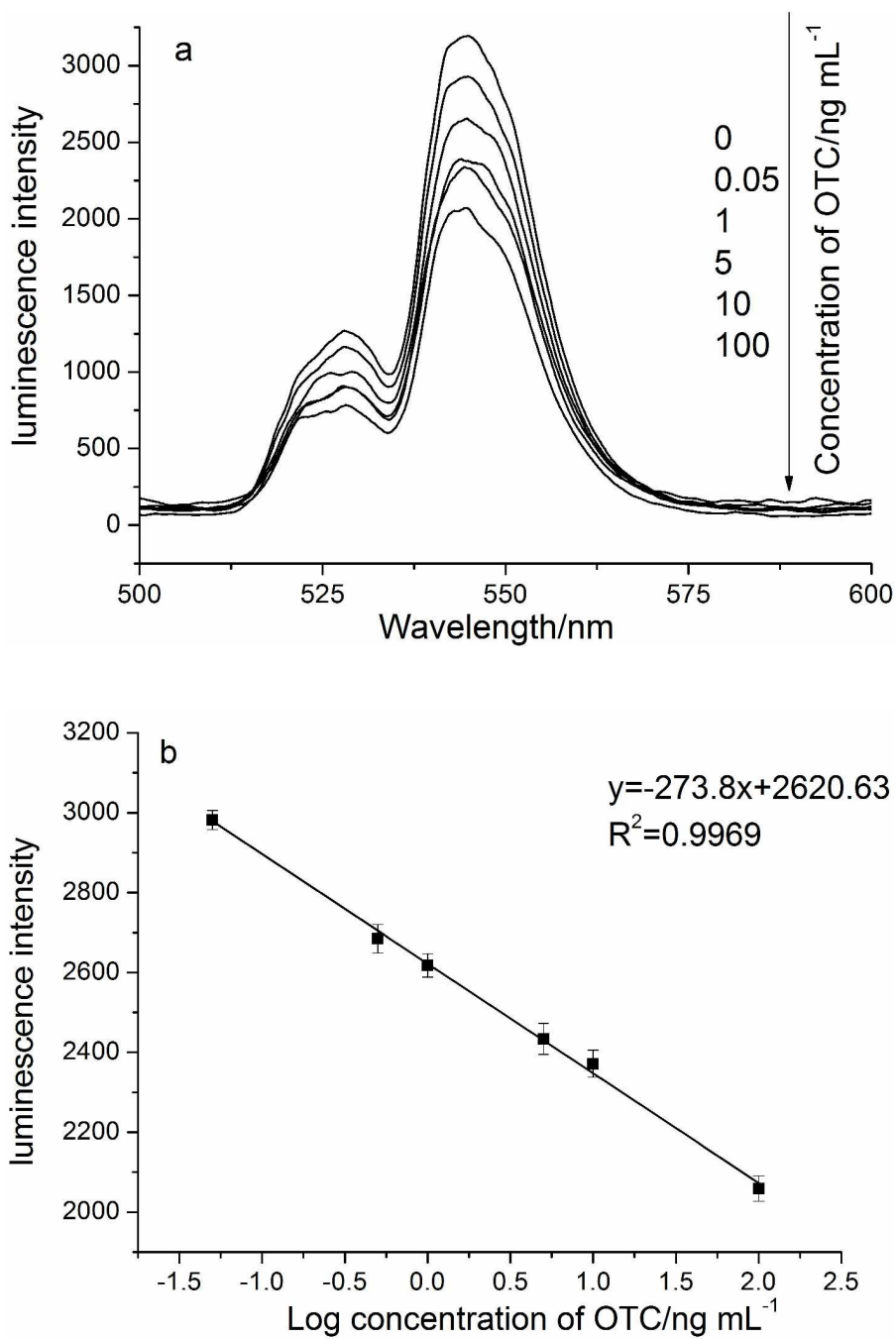


Fig.12 Typical recording output for the detection of different concentrations of OTC (a). Standard curve of the related upconversion luminescence intensity versus the concentrations of OTC (b)

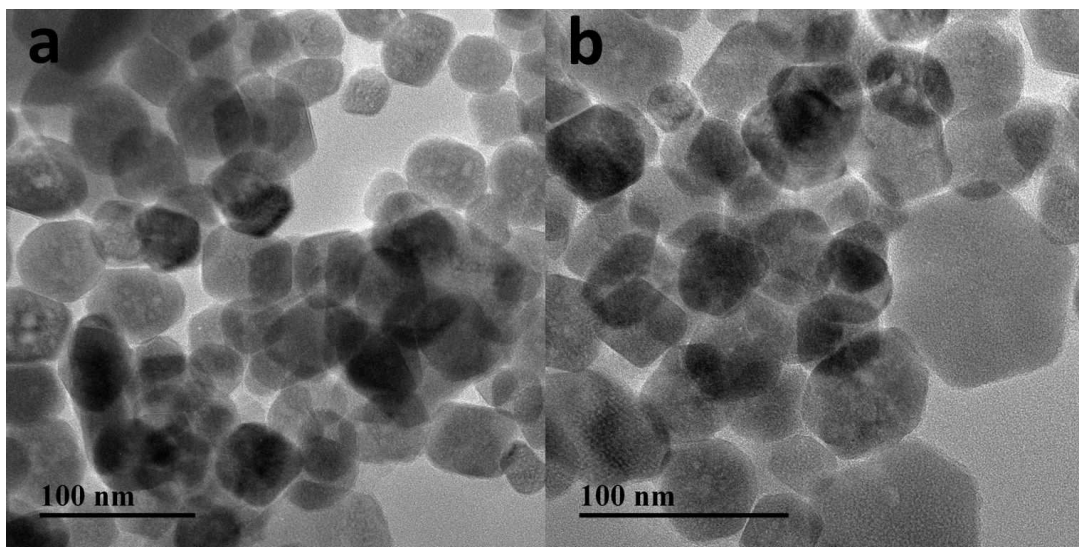


Fig. 13 TEM images of MNPs-UCNPs before (a) and after (b) target treating.

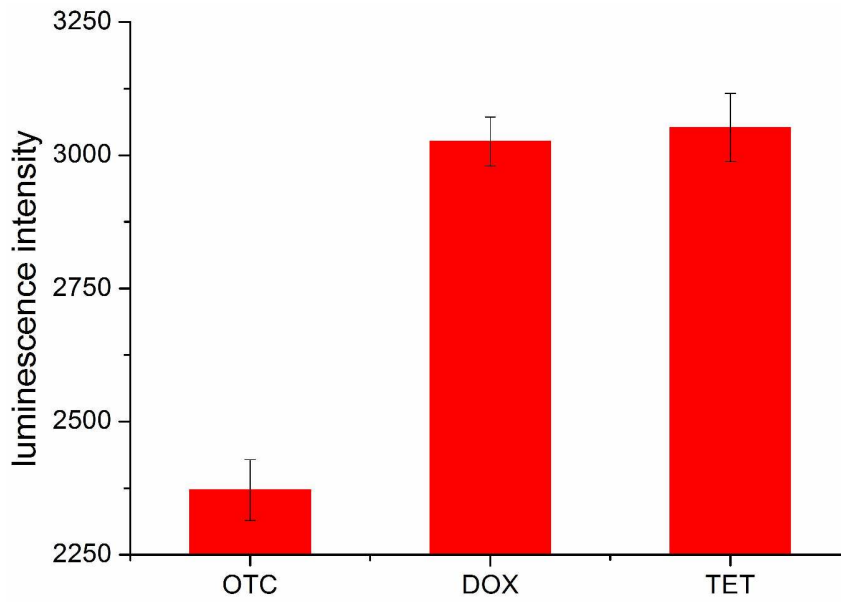


Fig. 14 Differential luminescence response of the aptasensor at 544 nm to OTC, DOX, and TET at the same concentration (10 ng mL^{-1})

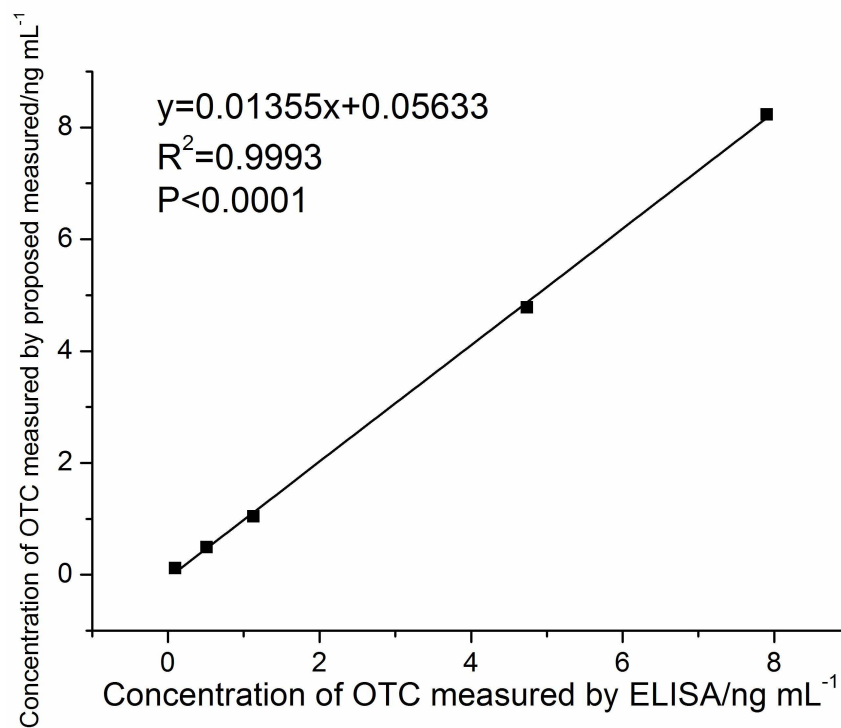


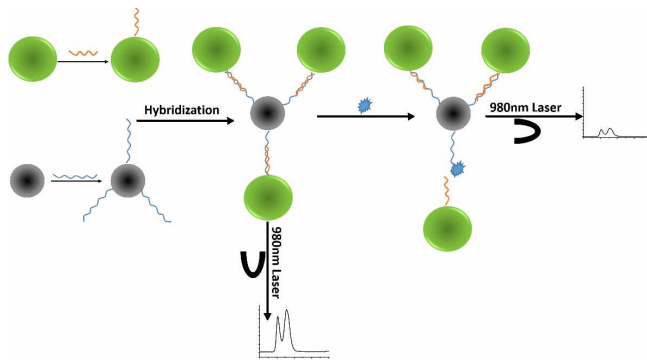
Fig. 15 Relationship between the proposed method and ELISA method for OTC detection

Table 1 The reported detection methods for OTA and the limit of detection

Methods	LOD	References
UHPLC method	0.2 / 0.003 ng ml ⁻¹	19
Method based on indirect competitive ELAA	12.3 ng ml ⁻¹	20
ELISA	7.01 ng ml ⁻¹	21
Electrochemical determination	0.1 μM	24
An electrochemical biosensor	9.8 ng ml ⁻¹	27
AuNP-based colorimetric assay	0.1 nM	29
Cantilever Array Sensors	0.2 nM	35
Fluorescent assay	10 nM	36

Table 2 Recovery results for the added standard OTC from milk samples obtained by the developed method

Sample	Background Content (ng ml ⁻¹)	Added Concentration (ng ml ⁻¹)	Detected Concentration (ng ml ⁻¹)		Recovery Ratio (%)
			ELISA	aptasensor	
1	0	0.1	0.093	0.119	119.00
2	0	0.5	0.512	0.493	98.60
3	0	1	1.127	1.042	104.20
4	0	5	4.738	4.782	95.64
5	0	8	7.901	8.232	102.75



Schematic illustration of the highly sensitive aptasensor for oxytetracycline based on upconversion and magnetic nanoparticles